

How structured are the representations in transformer-based vision encoders? An analysis of multi-object representations in vision-language models

Tarun Khajuria, Braian Olmiro Dias, and Jaan Aru

Institute of Computer Science, University of Tartu {tarun.khajuria@ut.ee, braian.d@gmail.com, jaan.aru@ut.ee}

Abstract. Forming and using symbol-like structured representations for reasoning has been considered essential for generalising over novel inputs. The primary tool that allows generalisation outside training data distribution is the ability to abstract away irrelevant information into a compact form relevant to the task. An extreme form of such abstract representations is symbols. Humans make use of symbols to bind information while abstracting away irrelevant parts to utilise the information consistently and meaningfully. This work estimates the state of such structured representations in vision encoders. Specifically, we evaluate image encoders in large vision-language pre-trained models to address the question of which desirable properties their representations lack by applying the criteria of symbolic structured reasoning described for LLMs to the image models. We test the representation space of image encoders like ViT, BLIP, CLIP, and FLAVA to characterise the distribution of the object representations in these models. In particular, we create decoding tasks using multi-object scenes from the COCO dataset, relating the token space to its input content for various objects in the scene. We use these tasks to characterise the network’s token and layer-wise information modelling. Our analysis highlights that the CLS token, used for the downstream task, only focuses on a few objects necessary for the trained downstream task. Still, other individual objects are well-modelled separately by the tokens in the network originating from those objects. We further observed a widespread distribution of scene information. This demonstrates that information is far more entangled in tokens than optimal for them to represent objects similar to symbols. Given these symbolic properties, we show the network dynamics that cause failure modes of these models on basic downstream tasks in a multi-object scene.

Keywords: Abstraction · Symbols · Vision-Language Models · Vision Encoder

1 Introduction

This study investigates whether symbol-like structured representations may emerge in transformer-based vision models. In vision models, some studies have evalu-

ated their representations, looking for aspects of human-like symbolic cognitive processes [19, 21]. An advantage of searching for symbolic representations in vision models is that the input information is distributed in pixels, allowing explicit binding dynamics to be observed. Binding dynamics refers to the information about entities (objects, living things, see Fig 1.C) being bound together into smaller representational units, describing specific useful aspects of that entity [9]. Further, in vision models, the intermediate representations of objects are natural candidates to be formed into symbols, allowing one to formulate hypotheses about the nature of the representations. Building upon the notion of symbols and binding described in previous studies [9, 19, 21], we propose three levels of properties for an image encoder representation to be more symbolic: 1) The model should be able to aggregate information specific to objects in the image into smaller units; 2) The model should represent various logical components of the input image in separate computational units, i.e., there should be object-wise information disentanglement; 3) A downstream processing network should be able to utilise the composition of these units for the required task, e.g., scene modelling for captioning.

The first two of these proposed properties of being symbol-like promote better out-of-distribution generalisation by themselves. 1) Better binding of object information into a discrete set of units allows useful properties of the representation to be fully available for novel scenarios in solving downstream task. 2) Disentanglement of these units of representation makes sure that the presence of one object does not affect the representation of others. This is important for extreme cases where the objects are present out of the scene statistics of the trained distribution and these spurious correlations in representations of object presence may cause failure for the downstream task.

The compositional abilities of these Vision-Language Models (VLMs) have already been tested and shown to be inadequate [28]. However, there is some evidence that while doing downstream tasks, primitive concepts emerge in model representations and are compositionally employed by the downstream network [29]. Transformers have already been shown to have global and local information aggregation within a single layer facilitated by the attention mechanism [24]. Also, due to the retention of the token space across layers, they could have enough computational units to maintain object information separately while binding them locally. Hence, there is a need to estimate the extent to which the first two properties of symbolic representations listed above are implemented in vision transformer models.

For this purpose, we analyse the spatial representations in the vision transformers’ token space. Our primary questions testing for properties 1 and 2 are the following: Do transformers represent and maintain object-wise representations? Are these representations disentangled, i.e. does a particular set of tokens only represent a particular object? We utilise the COCO dataset [17] with its instance object masks to characterise the token representations in relation to their input patch information. We set up decoding experiments in a two-object setting (in a multi-object scene) to determine how the encoders manage the representations

of the two objects. We try encoder of three VLMs (CLIP [23], BLIP [16] and FLAVA [25]) and compare them with the larger versions (CLIP-L, BLIP-L) and also check the representations against VIT trained for image classification and CLIP (Resnet X4) with a CNN backbone.

We generally observe that object-specific areas hold the most discriminative features about the objects until the last layers. The token representations are not disentangled since they can decode other objects in the scene with accuracy far above random guesses. Across networks, we see similar patterns of decoding accuracies in transformer-based VLMs. We observe the VLMs trained on objectives requiring the modelling of multiple objects have better symbol-like differentiated object representations than VIT encoders trained for image classification. On the other hand, all VIT-based encoders have less differentiated and disentangled object representation in CNN-based CLIP (Resnet X4). Our results suggest a preference for modelling objects relevant to the downstream task (e.g., captioning for BLIP). This effect is more pronounced for the CLS token directly optimised for the task; other object-specific tokens still retain more high-level information about most objects. We analyse and discuss the implications of representation loss in CLS for failure in out-of-distribution task scenarios.

2 Related Works

The overall problem with generalisation in DL methods and the need for explicit inductive biases that allow for discrete yet flexible information binding has been comprehensively discussed [9]. Discrete symbolic representations are considered a prerequisite for robust compositionality and reasoning [21] and new studies propose that such discrete information binding may originate from training existing models on large datasets [19, 21]. This issue carries over to the field of meta-learning with its aim to introduce and compositionally utilise modularity in neural networks to improve generalisation [13].

Concept bottleneck models are a series of models that try to explicitly learn human interpretable intermediate outputs to be composed into final output labels [7, 27]. This interpretability usually comes at the cost of downstream task performance. [11] introduced an extra loss in the intermediate layer on the networks for units to align to the interpretable concepts while preserving task performance. Many other works do not bind representations to any explicit intermediate concept but still have explicit discrete bottlenecks in their networks [18, 20]. It has been shown that these networks learn better representations which further help generalisation on downstream tasks [18, 20, 26].

2.1 Evaluating model’s reasoning capabilities

Many works have proposed benchmarks, and others have tried to analyse the existing networks to estimate the reasoning capabilities of the ANN models. [3] proposed a visual question-answering benchmark to evaluate the reasoning skills on images, with open-ended and free-form questions and expected solutions in

free-form natural language. Visual genome [12] provided content-rich images with explicit annotation of object position and relationships, promoting models that exploit such information. Datasets such as CLEVR [10] were designed to correct for biases the models would utilise in the existing benchmarks to perform well without explicit reasoning. The ARO (Attribute, Relation, Order) dataset [28] has been proposed to test the correct binding of information when compositionally representing multi-object scenarios. Particularly in VLMs such as BLIP and CLIP, they find that the model outputs do not bind the compositional properties well and attribute the wrong order and features to objects when describing them.

2.2 Interpreting model’s representations

In terms of analysis of model representations for concepts, early work [2] showed the layer-wise progression of decoding accuracy for concepts in CNNs. [6] reveals the inner workings of transformers by showing how trained transformers can implement convolutions and, in the initial layers, form grid-like local attention patterns like a convolution filter. [24] shows that vision transformers differ from CNNs because of their ability to encode both local and global information in the initial layer. Instead, in CNNs, there is a multi-scale feature representation going from lower-scale local information captured in the initial layers to higher-scale global information captured in the higher layers [4].

Particularly for vision-language models, [5] analysed various models trained using cross-model attention, providing insights into the attention patterns between the two modality streams and the relative contribution of each modality towards downstream tasks. Further, they found function-specific attention heads in the pre-trained models. VL Interpret [1] was designed as a visualisation tool to interpret the vision-language model’s instance-specific and aggregate statistics over attention distribution. Further, the tool helps visualise token representation as it passes through various network layers.

In contrast to the generic visualisation tools that look into the model’s functioning, many studies inspect their representations, evaluating a specific computational functionality. [14] finds modular subnetworks in trained ANN models functionally responsible for separate tasks. Multiple studies further look into the notion of concepts in trained vision-language model representations. One study [29] designed a test to check if primitive concepts emerge in the network’s representations, which are used compositionally for downstream tasks. [19] defines tests for concepts in visual representations according to Fodor’s criteria [8] and tests these criteria using a controlled synthetic dataset. In our work, we build on the intuitions from these works while trying to formulate our hypothesis about symbolic representations in a limited scope but testing it with images from natural scenes.

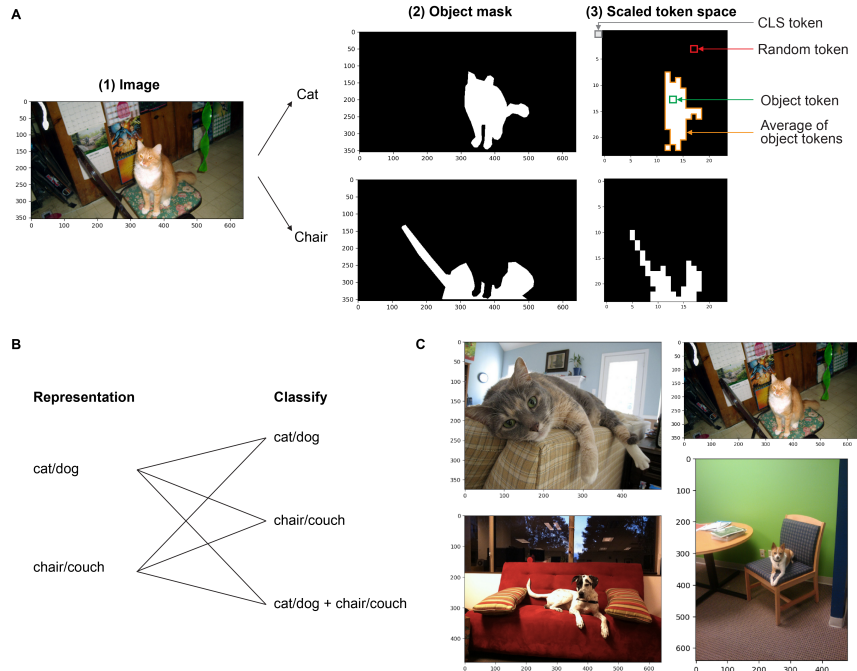


Fig. 1: A. Explanation of how the token representations are obtained. We analyse four kinds of tokens in this study 1) CLS token: Is common to both objects in the image; Object-specific 2) Avg_obj: obtained by averaging the token representations of the object-masked tokens as shown in the figure. 3) Random_obj (Object token): Rather than averaging, we sample one of the tokens from the masked token space of the object 4) Random : Obtained by sampling any random token from the token space other than the CLS token **B.** Describes the experimental setup in which we perform decoding in paired object tasks; each object-specific representation decodes 1) the object itself, 2) the other object in the image, and 3) the combination of both objects. **C.** Shows a sample paired object decoding task; given an image, the task is to decode if it contains object1 (cat/dog), object2 (chair/couch) or a combination of both.

3 Methods

We design probes and use similarity measures to evaluate the network’s representational structure. In the following section, we describe the details of the experimental setup, data and the networks analysed.

Experimental Setup: We decode the combination of objects in the image from a single token or an average of tokens obtained from various parts of the image (see Fig. 1.A). The tokens we are interested in include the 1) CLS token (the token used and trained for the downstream task), 2) Average token (avg_obj): the average of token representation obtained from the object, 3) Random object (random_obj) token: a single token randomly sampled from the object 4) Random token (Random): a randomly sampled token from the image that served as a baseline. The token representation is obtained at the output of each layer. In this process, to identify the tokens originating from an object, we scale the segmentation mask of the object to the size of the token space. The probing task is designed as a classification task with the following settings: we use the tokens originating from 1) Primary object, 2) Secondary object and use it to decode 1) Primary object category, 2) Secondary object category, 3) Combination of primary and secondary object categories (see Fig. 1.B). We train and evaluate the probes with a train/val/test setup with 80/10/10 percent data splits. The reported accuracies are all final test set accuracies. All trained probes are linear and use the Scikit-learn [22]’s perceptron implementation, with its default parameters. To check the baseline performance of these representations to decode objects in a complex (20 classes) task, we train layer-wise global object classification probes for each layer of the networks. These probes utilise first 40000 images from the MSCOCO train set for training the probes and the 5000 images in the validation set for testing. To make the linear probe with less learning capacity, we use only the top 20 frequent object categories in the 40000 training images in the probing task.

Dataset: We needed instance segmentation masks to associate the tokens to the object in the image. Hence we used the COCO dataset and created subsets with enough combination of two object categories co-occurring in them. We then excluded images with more than one object category of primary or secondary objects. While choosing the objects across primary and secondary categories we preferred objects more likely to interact in the scene. Within the primary and secondary categories we preferred objects that are similar to each other, so their embedded representations are not naturally distinct, increasing our probe’s sensitivity. We used six task sets with a total of 16,288 images. For example, the first task contains a combination of objects from two sets, i.e. a primary object: animal (cat/dog) and a secondary object: furniture (chair/bench/bed/couch). The dataset and its tasks are detailed in Table 1. We call this set of tasks ‘object pair decoding tasks’. The global probes were trained and tested on a larger dataset. We selected the first 40000 images in COCO’s training set for training and the 5000 images in the validation set for testing.

Linear Probing: We probe the representations in pre-trained networks for our analysis. Probing an information system involves obtaining a representa-

Table 1: For paired object decoding, we use 6 tasks with different number of images in each task. Each task contains images with different variations of objects

	Task1	Task2	Task 3	Task4	Task 5	Task 6
# Images	2414	5042	1953	2143	938	3738
Objects 1	cat, dog	dining table, person	train, bus	tv, laptop	microwave, oven	motorcycle, car
Objects 2	bench, chair, couch, bed	pizza, knife, cup, cake	traffic light, bench, backpack, handbag	mouse, remote, keyboard, cellphone	bottle, spoon, knife, cup	traffic light, handbag, backpack, bicycle

tion, usually in the form of a vector from the system in response to an image. Then, we estimate if that particular vector can classify information about the stimuli correctly. The kind of information the probe can learn to classify and the complexity of the probe (i.e. is it just a linear classifier or a complex multilayer NN) indicates the nature of information present in that layer’s representation. We obtain representations from various parts (layers and spatial sections tokens/cells) of the network and use them to understand the network by looking at the classification ability of a linear probe.

Analysed Networks: We analysed the image encoders of seven models: BLIP (ViT-B/16 and ViT-L/14) model for image captioning, CLIP for image-text matching, FLAVA model with an additional multimodal encoder on top of vision and language encoders and finally, ViT-B/16 encoder trained on imagenet21k image for image classification task. We analysed both ViT B/16 and L/14 (Image Transformer) and the Resnet X4 (CNN) image encoder for the CLIP. In CNN analysis, we obtained feature cells instead of tokens, i.e., we used the vector representation of a cell in the feature map by accumulating all the filter outputs at the cell location. In both transformers and CNNs, the place on the feature map representing the object is computed by scaling the object segmentation map to the size of the feature map at the layer. The images are pre-processed with the standard pre-processing function and setting provided along with the pre-trained network instances.

4 Results

4.1 A snapshot of network’s global and image-specific representation

Decoding the objects in a multi-object scene using the trained model’s representations gives us a picture of how the information about the scene is organised in the network. In our study, we have used two kinds of decoding tasks (object-paired tasks and global decoding tasks) to estimate the architecture-level organ-

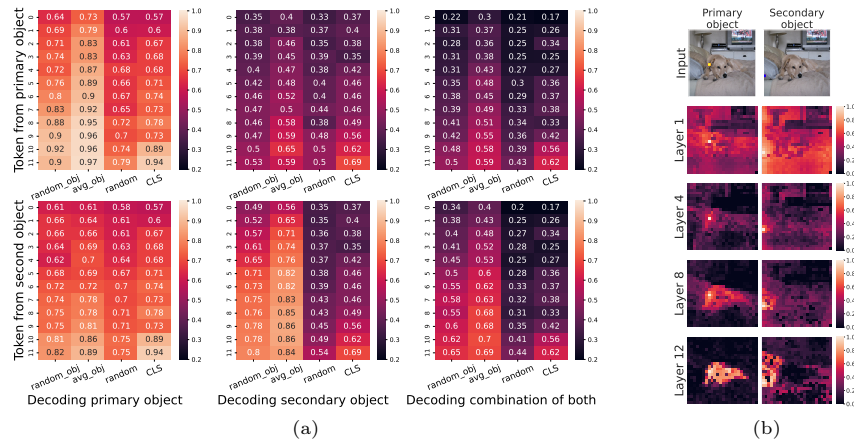


Fig. 2: **a.** Object-pair decoding task results for BLIP: Average decoding performance for different layers (y-axis) and token types (x-axis) over 6 tasks for BLIP. In the sub-figures, the y-axis contains variations of where the object-specific tokens (`random_obj` and `avg_obj`) are obtained. The different columns show results for 1) decoding the primary object 2) the secondary object 3) the combination of both objects in the image. The decoding pattern remains after averaging, with the tokens from the objects modelling the most useful information for categorising the objects. They are much better than the CLS token, which has to capture the larger scene context. **b.** Visualisation of cosine similarity to other tokens for a token from primary and secondary object.

isation of these representations. We also generate representation similarity maps to analyse the representation of a single image in a particular model.

Using the paired object decoding tasks, we can see that the objects in the network can be linearly decoded considerably above random accuracy by using a single token representation originating from the object or by using an average of token representations from the object. The general trend followed by these decoding accuracies can be seen in Fig 3. The global object decoding probes, with their 20 class classification setting, provide a good baseline of the ability of the token’s representations to decode between multiple objects. The high correlation of these accuracies for each network (see Fig. 4) to paired-object classification tasks’ results shows that the accuracies are not obtained due to an easy 2-way or 4-way classification task set up in the paired object tasks.

Finally, in Fig. 2, you can see the detailed results for decoding accuracies for the four types of token representation used in our analysis for the paired object decoding tasks. This provides a more detailed global picture of the model’s representations of object pairs from the images. For an instance-wise image-level analysis of representations, we generate similarity maps of the object representations that show how a particular token’s relation to other tokens changes across layers in the model for a particular image. In 2.b, an image shows a representation similarity map for two tokens in an image 1) from the primary object 2) from the secondary object. One can notice how the representations of tokens

originating from the same token start having similar representations as we move toward the upper layers. The tokens from the primary object acquire similar representation, but for the secondary object, many tokens that are outside the object also have high cosine similarity in the last layer.

4.2 How different token representations encode objects, their interaction and their importance

In the paired-object tasks, the images consist of a primary object and a secondary object. We see the representation of these two object combinations in each image in four type of token representations from the models. Based on the results from the BLIP model shown in Fig 2 we now discuss the general trend of representations across models. Specific differences are discussed in subsection 4.3.

In our results (see Fig. 4), in all pre-trained models, the primary objects are decoded equally well by the CLS token as the average token representation of the object. There is a decrease in decoding accuracy from primary to secondary object categories. This is partially due to the added complexity of a 4-way classification in the secondary object. However, the CLS token decodes the secondary objects with much less accuracy than both the object-specific tokens (avg_obj and random_obj). The CLS tokens that are optimised for the downstream tasks in each of these networks are expected to model the best information about the scene. But this also means that not all objects are linearly decodable by the CLS token. We observe that the object-specific tokens have better object decoding accuracy as compared to the CLS token (In BLIP Fig 2 primary object CLS:0.94 vs Avg_Obj: 0.97 and secondary object CLS: 0.69 vs Avg_Obj: 0.84). There is a particular degradation in decoding performance using the CLS token for secondary objects, where the accuracy for the CLS token is far below the decoding accuracy of object-specific tokens (avg_obj and random_obj).

Previous analysis showed that the object-specific tokens have the highest accuracy for decoding the particular object from which they originated. Still, they also have high decoding accuracy for the other objects in the image. This accuracy is far above random guess and allows these tokens to decode a combination of objects in the current image (see Fig. 2, for results on BLIP). The final decoding accuracy for the combination is 0.59 when using the primary (avg_obj) object token and 0.69 when using the secondary one. In Fig. 2, one can notice that the primary avg_obj token is much worse at representing the secondary objects than the other way around. These results have implications for the disentanglement of these object-specific tokens. Further, the CLS token also shows a decent decoding accuracy as it is optimised to capture more global information from the image. This accuracy is not higher than the object-specific secondary tokens due to its poor capturing of information about these secondary objects in the scene (CLS token decoding accuracy for the secondary object is 0.69 compared to 0.94 for the primary object, as seen in Fig. 2).

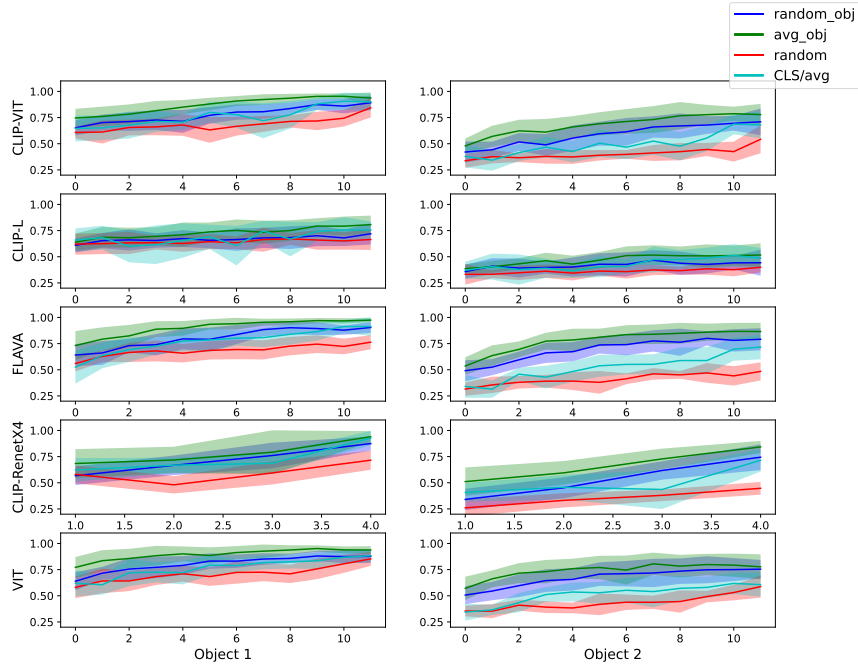


Fig. 3: Layer-wise test set decoding accuracy for primary and secondary objects for five pre-trained models in the study. Results for all models are shown in appendix. The accuracies are averaged over the six task sets. In each sub-graph, the y-axis denotes the decoding accuracy and the x-axis denotes the layer at which the accuracy was observed. We observe consistent decoding trends across models with a few variations reported in 4.3.

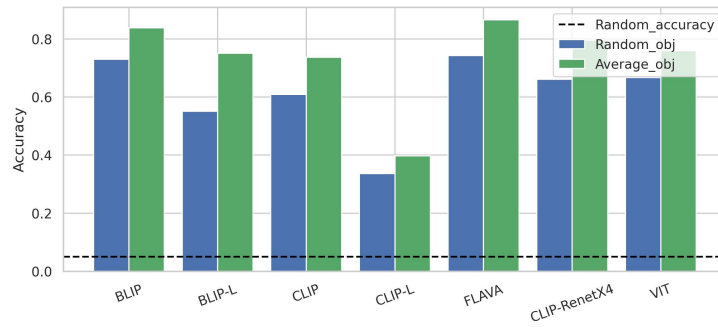


Fig. 4: Results from global image probes: Final layer test set decoding accuracy for 20 object classes for all pre-trained image encoders in the study. We observe that all networks perform way above average using a linear readout for a more difficult 20-class classification task.

4.3 VLM models trained on multi-object images have more modular representations than ViT (trained for single object classification)

In this section, we compare the representations of the models with each other. For the global decoding task, we see that the newer VLMs like FLAVA and BLIP have higher decoding accuracy with their object-specific representations than the other counterparts like CLIP (see Fig 4). Larger models like CLIP-L and BLIP-L counterintuitively perform worse than their base counterparts. Specifically, CLIP-L shows fairly lower decoding accuracy for both single random object and average object token representation (random_obj and Average_obj). In the paired-object decoding tasks, the VLM models follow the overall trend of decoding accuracy being correlated to the results in the global object probing tasks (see 3). The relative accuracy trends for various tokens are similar across VLM models. The notable observation is the higher overall decoding performance of FLAVA models, which also shows a higher differentiation of object-wise representations, i.e the random token accuracy is fairly lower in the last layer compared to object-specific tokens.

We observe a difference in the structure of representations due to architecture (Transformer vs CNN) and specific training on multi-object tasks i.e ViT vs other models. Hence, we observe a significant decrease in decoding accuracy using the random CNN unit representation compared to random ViT tokens (In the last layers, primary object ViT: 0.84 vs CNN: 0.72; secondary object ViT: 0.54 vs CNN: 0.45)(see 3). Further, the object-specific tokens in CNNs have lower accuracy while decoding the other objects than their ViT counterpart (In the last layers, primary object ViT: 0.88 vs CNN: 0.8; secondary object ViT: 0.6 vs CNN: 0.59). This indicates that CNN has less entanglement of object-specific information across objects than the ViT counterpart in CLIP. We attribute these results to CNNs not having the ability for the information to travel across units in each layer, hence the object information remains more localised. ViT trained on ImageNet21k shows the least differentiation between object-specific and other tokens as compared to the other Transformer models. Here a random token decoded the object with almost similar accuracy as compared to the CLS token (see Fig. 3). And tokens from one object and similarly decode the category of other objects in the scene. Hence it seems like the scene-level information is more uniformly dispersed in the representations of ViT tokens trained only on single object classification task. This is in comparison to all the ViT models trained on tasks requiring modelling of more than one object for a correct representation of the information required for downstream tasks like text matching, captioning etc. Further, the differentiation of object-specific token and consequently the disentanglement of information is more explicit in these networks than ViT.

4.4 Special tokens may not be special for your downstream task with multi-object images

Following the observations about the lower decoding accuracy of secondary objects using CLS tokens, we wanted to check if the low accuracy results from the

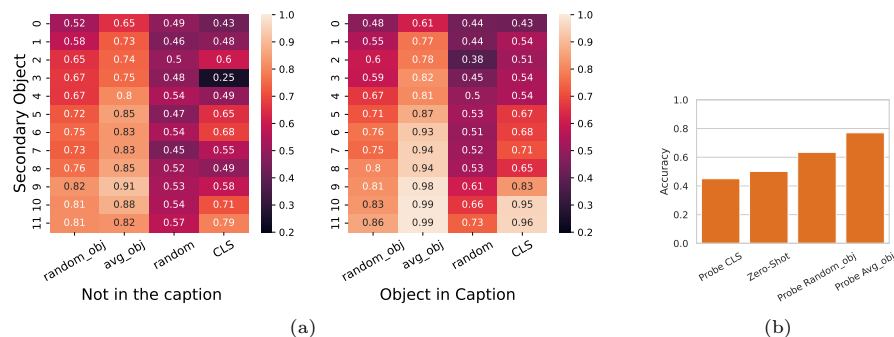


Fig. 5: **a.** Variation in decoding accuracy between instances of objects ‘in caption’ and ‘not in caption’. Each subplot represents the decoding of the object by its object-specific representation. **b.** Object detection accuracy on test set using probes trained on three different token representations from CLIP and zero-shot CLIP accuracy.

object’s importance in the downstream task (captioning in the case of BLIP). Hence, we analysed the decoding accuracy for two sets of data. The set was divided based on whether the object was directly mentioned in the caption generated by the model. Due to this split, we rejected tasks with less than 400 samples in either of the new sets. Therefore, we are left with 3 tasks whose average results are reported in Fig. 5a. In our results in Fig. 5a, we report a decrease in decoding accuracy of the objects not mentioned in captions using all kinds of tokens considered in our analysis (Average final layer accuracy for primary object, which was for ‘in caption’: CLS:1 and avg_token: 0.99, drops to CLS: 0.87 and avg_obj 0.93 when the object is ‘not in caption’. In the secondary object, the drop is from ‘in caption’: CLS: 0.96 and avg_obj: 0.99 to ‘not in caption’: CLS: 0.79 and avg_obj: 0.82). This means the network pays more attention to certain objects, and its learning of discriminative features deteriorates for objects not mentioned in the captions. We note that the decrease in the decoding is most pronounced for the CLS token, showing the direct effect of the downstream task on the representation.

We further use this understanding to check for failure in zero shot object detection (i.e. retrieval) tasks using CLIP in a multi-object setting. We use the classification task setting for the global probe. We use the object-specific representation using 1 token and avg_obj token to learn probe to classify the top 20 objects in test set images. Then we evaluate the CLIP zero shot performance to detect objects in the image using the prompt ‘An image containing a ‘category’’. Where the category was replaced with 20 candidate objects. We finally evaluate the accuracy of finding the objects. A fourth multi-class object detection probe is learnt using the CLS token representation. As we compare the accuracy of these four methods on the simple object retrieval task, we find that the probes using the average patch representation gives the best accuracy followed by random_obj token and zero shot model accuracy and multi-class probe (See Fig. 5b).

5 Discussion

In this work, we started by identifying three characteristics required in representations of image models for them to be symbol-like: 1) The architecture should be able to aggregate information specific to objects on the image into smaller units; 2) The architecture should represent various logical units of the input image in separate computational units, i.e., there should be object-wise information disentanglement; 3) A downstream processing network should be able to utilise the composition of these units for the required task.

Most vision encoders fulfill the first criterion we described as they aggregate useful information from the image into smaller representation space useful for the downstream task. However, we were interested in whether separate representational units specialise in representing the image’s separate constituent parts (objects). Our analysis shows that the object-specific (`avg_obj`, `random_obj`) tokens show decent decoding accuracy across the models. Each object-wise token’s accuracy for classifying itself is our estimate for fulfilling this criterion. For the second characteristic, we looked at the network’s capability to form disentangled representations of objects. We saw evidence that the information about other objects also leaks into the object-wise representations. Ideally, each object representation can only decode that particular object and other objects in the scene cannot be decoded by that representation. As the other objects can be decoded in our object representations (with accuracies of 0.89 by secondary object representations and 0.65 by primary object representations), their representations are already affected by the context, i.e. other objects. This finding implies that the downstream task using these representations compositionally still cannot perform structured composition as with abstract symbols. Further, the higher the decoding accuracy of other objects in the scene, the higher the entanglement in the representation. The entangled object representation will affect the downstream network’s outputs if the context information is irrelevant to the task.

Our comparative analysis of the BLIP model’s performance showed a notable degradation in decoding efficacy across all representations when objects were omitted from its captions. This observation underscores the significant influence of the model’s downstream objective on its representational capabilities. On the one hand, this enhances the disentanglement of object representations, reducing interference from objects insignificant to the task. Conversely, it reduces the model’s generalizability, particularly when deployed in diverse tasks or faced with unfamiliar input distributions. Our results show that this problem is most exacerbated in the representation of the CLS token. Most research predominantly assesses these networks’ capabilities based on their final outputs, which rely on representations like a CLS token (for example in [15,28]). Our findings show a loss in representing multiple objects during this process of funneling information into the CLS token. Further, the downstream objective’s effect is the most extreme on the nature of these representations. We show that this causes suboptimal performance of these networks in simple tasks such as retrieval in the multi-object setting. We further postulate that these phenomena (non-binding

of certain objects representations or entangled representations) significantly contribute to the models’ suboptimal performance in tasks that require to compose using the representation of objects in scenarios involving multiple objects. In evaluations of CLIP, FLAVA and similar models within a multi-object context, the ramifications of the CLS token bottleneck and its training procedure (training data and objective) must be meticulously considered. The objects represented and the nature of their representation in this bottleneck are heavily influenced by the downstream objective or a co-occurring object, thereby affecting the accuracy of outputs in tasks that diverge from the types of instances encountered during training. Future work can utilise our method to look into training better readouts and fine-tuning on specific underrepresented object images.

6 Limitations

The probing and representation analysis methods we used in our analysis have some limitations, and the results must be carefully interpreted. High decoding accuracy in a decoding task with two or four objects may be due to the easy decoding task (if the object classes are naturally distinct and it is only a 2/4 way classification). Further, the fact that one can classify a particular object from a few other classes may depend on representing a single or a few features distinguishing between the classes. This representation may not model many other aspects of the object. We controlled for this limitation by training global probes for 20-class classification using the same representations, showing reasonably high accuracy. Likewise, a lower decoding accuracy does not mean that the model does not have information about the particular object; the information is just not encoded with linear distinction at that layer/token. Overall, we are averaging over six tasks in many object categories. Hence, even though the exact numbers may not reflect the model’s exact state, the relative numbers are helpful in making inferences about the model and its representations.

7 Conclusion

In this work, we first formulated three characteristics for symbolic representations in an image encoder. We then analysed the representations of transformer-based image encoders in ViT, BLIP, CLIP, FLAVA and CLIP (Resnet X 4) image encoders. Through probing tasks, we observed that object-specific areas hold the most discriminative features about the objects until the last layers. Their discriminative ability decreased when the objects were not important for the downstream task but was still reasonably maintained. The token representations are not disentangled since they can decode other objects in the scene with accuracy far above random guesses. We found that the aggregate image representation, i.e. CLS token for transformers, does not represent all objects, and its discriminative ability degrades the most when the object is not useful for the trained downstream task. Our work thus characterises the extent to which the representations of these image encoders are symbolic and gives insights into

the failures on out-of-distribution downstream tasks that utilise the composition of these features.

References

1. Aflalo, E., Du, M., Tseng, S.Y., Liu, Y., Wu, C., Duan, N., Lal, V.: VI-interpret: An interactive visualization tool for interpreting vision-language transformers. In: Proceedings of the IEEE/CVF Conference on Computer Vision and Pattern Recognition. pp. 21406–21415 (2022) [4](#)
2. Alain, G., Bengio, Y.: Understanding intermediate layers using linear classifier probes. arXiv preprint arXiv:1610.01644 (2016) [4](#)
3. Antol, S., Agrawal, A., Lu, J., Mitchell, M., Batra, D., Zitnick, C.L., Parikh, D.: Vqa: Visual question answering. In: Proceedings of the IEEE international conference on computer vision. pp. 2425–2433 (2015) [3](#)
4. Bronstein, M.M., Bruna, J., Cohen, T., Velicković, P.: Geometric deep learning: Grids, groups, graphs, geodesics, and gauges. arXiv preprint arXiv:2104.13478 (2021) [4](#)
5. Cao, J., Gan, Z., Cheng, Y., Yu, L., Chen, Y.C., Liu, J.: Behind the scene: Revealing the secrets of pre-trained vision-and-language models. In: Computer Vision–ECCV 2020: 16th European Conference, Glasgow, UK, August 23–28, 2020, Proceedings, Part VI 16. pp. 565–580. Springer (2020) [4](#)
6. Cordonnier, J.B., Loukas, A., Jaggi, M.: On the relationship between self-attention and convolutional layers. arXiv preprint arXiv:1911.03584 (2019) [4](#)
7. De Fauw, J., Ledsam, J.R., Romera-Paredes, B., Nikolov, S., Tomasev, N., Blackwell, S., Askham, H., Glorot, X., O’Donoghue, B., Visentin, D., et al.: Clinically applicable deep learning for diagnosis and referral in retinal disease. *Nature medicine* **24**(9), 1342–1350 (2018) [3](#)
8. Fodor, J.A.: Concepts: Where cognitive science went wrong. Oxford University Press (1998) [4](#)
9. Greff, K., Van Steenkiste, S., Schmidhuber, J.: On the binding problem in artificial neural networks. arXiv preprint arXiv:2012.05208 (2020) [2](#), [3](#)
10. Johnson, J., Hariharan, B., Van Der Maaten, L., Fei-Fei, L., Lawrence Zitnick, C., Girshick, R.: Clevr: A diagnostic dataset for compositional language and elementary visual reasoning. In: Proceedings of the IEEE conference on computer vision and pattern recognition. pp. 2901–2910 (2017) [4](#)
11. Koh, P.W., Nguyen, T., Tang, Y.S., Mussmann, S., Pierson, E., Kim, B., Liang, P.: Concept bottleneck models. In: International conference on machine learning. pp. 5338–5348. PMLR (2020) [3](#)
12. Krishna, R., Zhu, Y., Groth, O., Johnson, J., Hata, K., Kravitz, J., Chen, S., Kalantidis, Y., Li, L.J., Shamma, D.A., et al.: Visual genome: Connecting language and vision using crowdsourced dense image annotations. *International journal of computer vision* **123**, 32–73 (2017) [4](#)
13. Lake, B.M., Baroni, M.: Human-like systematic generalization through a meta-learning neural network. *Nature* pp. 1–7 (2023) [3](#)
14. Lepori, M.A., Serre, T., Pavlick, E.: Break it down: evidence for structural compositionality in neural networks. arXiv preprint arXiv:2301.10884 (2023) [4](#)
15. Lewis, M., Yu, Q., Merullo, J., Pavlick, E.: Does clip bind concepts? probing compositionality in large image models. arXiv preprint arXiv:2212.10537 (2022) [13](#)

16. Li, J., Li, D., Xiong, C., Hoi, S.: Blip: Bootstrapping language-image pre-training for unified vision-language understanding and generation. In: International Conference on Machine Learning. pp. 12888–12900. PMLR (2022) [3](#)
17. Lin, T.Y., Maire, M., Belongie, S., Hays, J., Perona, P., Ramanan, D., Dollár, P., Zitnick, C.L.: Microsoft coco: Common objects in context. In: Computer Vision–ECCV 2014: 13th European Conference, Zurich, Switzerland, September 6–12, 2014, Proceedings, Part V 13. pp. 740–755. Springer (2014) [2](#)
18. Locatello, F., Weissenborn, D., Unterthiner, T., Mahendran, A., Heigold, G., Uszkoreit, J., Dosovitskiy, A., Kipf, T.: Object-centric learning with slot attention. *Advances in Neural Information Processing Systems* **33**, 11525–11538 (2020) [3](#)
19. Lovering, C., Pavlick, E.: Unit testing for concepts in neural networks. *Transactions of the Association for Computational Linguistics* **10**, 1193–1208 (2022) [2](#), [3](#), [4](#)
20. Oord, A.v.d., Vinyals, O., Kavukcuoglu, K.: Neural discrete representation learning. *arXiv preprint arXiv:1711.00937* (2017) [3](#)
21. Pavlick, E.: Symbols and grounding in large language models. *Philosophical Transactions of the Royal Society A* **381**(2251), 20220041 (2023) [2](#), [3](#)
22. Pedregosa, F., Varoquaux, G., Gramfort, A., Michel, V., Thirion, B., Grisel, O., Blondel, M., Prettenhofer, P., Weiss, R., Dubourg, V., et al.: Scikit-learn: Machine learning in python. *the Journal of machine Learning research* **12**, 2825–2830 (2011) [6](#)
23. Radford, A., Kim, J.W., Hallacy, C., Ramesh, A., Goh, G., Agarwal, S., Sastry, G., Askell, A., Mishkin, P., Clark, J., et al.: Learning transferable visual models from natural language supervision. In: International conference on machine learning. pp. 8748–8763. PMLR (2021) [3](#)
24. Raghu, M., Unterthiner, T., Kornblith, S., Zhang, C., Dosovitskiy, A.: Do vision transformers see like convolutional neural networks? *Advances in Neural Information Processing Systems* **34**, 12116–12128 (2021) [2](#), [4](#)
25. Singh, A., Hu, R., Goswami, V., Couairon, G., Galuba, W., Rohrbach, M., Kiela, D.: Flava: A foundational language and vision alignment model. In: Proceedings of the IEEE/CVF Conference on Computer Vision and Pattern Recognition. pp. 15638–15650 (2022) [3](#)
26. Träuble, F., Goyal, A., Rahaman, N., Mozer, M.C., Kawaguchi, K., Bengio, Y., Schölkopf, B.: Discrete key-value bottleneck. In: International Conference on Machine Learning. pp. 34431–34455. PMLR (2023) [3](#)
27. Yi, K., Wu, J., Gan, C., Torralba, A., Kohli, P., Tenenbaum, J.: Neural-symbolic vqa: Disentangling reasoning from vision and language understanding. *Advances in neural information processing systems* **31** (2018) [3](#)
28. Yuksekgonul, M., Bianchi, F., Kalluri, P., Jurafsky, D., Zou, J.: When and why vision-language models behave like bags-of-words, and what to do about it? In: The Eleventh International Conference on Learning Representations (2022) [2](#), [4](#), [13](#)
29. Yun, T., Bhalla, U., Pavlick, E., Sun, C.: Do vision-language pretrained models learn composable primitive concepts? *arXiv preprint arXiv:2203.17271* (2022) [2](#), [4](#)